Journal of Global Positioning Systems (*2021*)
Vol. 17, No. 1: 34-47
DOI: 10.5081/jgps.13.1.34

BDS Real-time Satellite Clock Offsets Estimation with Three Different Datum Constraints

Guanwen Huang[1], Wei Xie[1*], Wenju Fu[2], Pingli Li[3], Haohao Wang[1] and Fan Yue[1]

1. College of Geology Engineering and Geomatics, Chang'an University, Xi'An 710054, China.
2. State Key Laboratory of Information Engineering in Surveying, Mapping and Remote Sensing, Wuhan University, Wuhan 430079, China.
3. The 20th Research Institute of China Electronic, Technology Group Corporation, Xi'An 710068, China.

* Correspondence: chdxiewei@chd.edu.cn

Abstract A clock offset datum should be selected to separate the satellite and receiver clock offset when estimating the Global Navigation Satellite System (GNSS) satellite clock offset. However, the applicable conditions and performance of the estimated satellite clock offset vary for different clock offset datums. In this paper, the BeiDou Navigation Satellite System (BDS) real-time satellite clock offset is estimated by using the undifferenced (UD) model with three datum constraints: receiver clock datum, satellite clock datum, and zero-mean condition (ZMC) datum. The constraint conditions of three clock offset datums are discussed, the transformation relationship among the three datums constraints is derived, and the characteristics of three clock offset datums are analyzed. One hundred stations were used to perform the experiments, and the results show mean standard deviation (STD) values of ±0.118, ±0.124, and ±0.101 ns for the receiver clock, satellite clock, and ZMC datum, respectively. The mean clock offset model precisions with the three datum are ±0.497, ±0.646, and ±0.442 ns, respectively. The frequency stability with ZMC datum results showed the best performance when the integration time is less than 10,000 s. For precise point positioning (PPP), the ZMC datum results show better performance among the three datum constraints. This study can provide a reference for clock offset datum selection for GNSS satellite clock offset estimation.

Keywords: Clock offset datum;·Receiver clock datum;·Satellite clock datum;·ZMC datum;·Satellite clock offset estimation; Satellite Clock performance

1 Introduction

The real-time satellite clock offset is one of the key elements for real-time precise point positioning (RT-PPP) and satellite clock performance monitoring and evaluation. PPP technology has been demonstrated as an effective tool that can be used in areas such as GNSS meteorology [Lu, et al, 2015], precise orbit determination of low earth orbit (LEO) satellites [Bock, et al, 2002], time and frequency transfer [Defraigne, et al, 2015], precision agriculture [Guo, et al, 2018], earthquake and tsunami early warning. Satellite clock performance monitoring is significantly crucial for satellite clock offset prediction, satellite clock offset estimation and integrity monitoring of satellite [Xie, et al, 2019].

The development of Chinese BeiDou Navigation Satellite System (BDS) followed the 'three-step' strategy. The first phase was the demonstration system (BDS-1) established in 2003, in which three geostationary orbits (GEO) satellites were launched. The BDS regional navigation satellite system (BDS-2) was established on 27 December 2012. A constellation

of 14 satellites, including five GEO satellites, five inclined geosynchronous orbits (IGSO) satellites, and four medium earth orbit (MEO) satellites were launched [Yang, et al, 2019]. The BDS-3 was completed on 31 July 2020. It contains 30 satellites, which can provide global positioning, navigation, and timing (PNT) services, and whose quality is based on the performance of the real-time satellite clock.

The atomic clock equipped on a navigation satellite is easily affected by the external environment and its characteristics, it is difficult to use the mathematical model for prediction. Therefore, the real-time satellite clock offset should be estimated using the ground observation stations, and the satellite and receiver clock offset parameters are estimated simultaneously when estimating the satellite clock offsets. There is a linear dependency relationship between the satellite and receiver clock offset, resulting in rank deficiency in the observation equations. Therefore, one clock offset datum should be selected to eliminate the rank deficiency [Liu et al., 2019]. The clock offset datum is the precondition that ensures the stability and continuity of the clock offset datum. Once the clock offset datum is missing or interrupted, the clock offset cannot be estimated. In previous studies on clock offset datum selection, Jiang et al. [2019) estimated the satellite clock offsets by using the ZMC datum to separate satellite and receiver clock offsets, and Fu et al. [2018) selected a receiver clock as a time reference when performing the GPS/BDS satellite clock estimation. By employing three different kinds of reference stations, internal cesium; external cesium; and external hydrogen-maser, as clock offset datum when conducting satellite clock estimation[Kamil et al. 2019]. Furthermore, Chen et al. [2018] applied one satellite clock as a clock offset datum to estimate the GPS/BDS/Galileo satellite clock offset. However, the transformation relationship and characteristics of three clock offset datums have not been discussed. Furthermore, the satellite clock performance comparison among the estimated real-time satellite clock offset estimations with three different datum constraints has not been reported.

In this paper, we focus on BDS real-time satellite clock offset estimation with three different datum constraints including one receiver clock datum, one satellite clock datum, and the ZMC datum. BDS real-time satellite clock offset estimation with three datum constraints was conducted, and the satellite clock performance of the estimated clock offset was compared by using three datum constraints. This study is organized as follows: after this introduction, the observation and functional model is introduced, and the constraint condition and transformation relationship of three clock offset datums are discussed. Then, the characteristics of the three datum constraints are analyzed. Next, the BDS real-time satellite clock offset estimation experiments with three datum constraints are conducted, and the clock performance in terms of clock offset accuracy, clock offset model precision, frequency stability, and PPP for three different clock offset datums are compared and analyzed. Finally, the conclusions are presented.

2 Methodology

In this section, the undifferenced (UD) observation and functional model are introduced. Then, the constraint conditions of the satellite clock, receiver clock, and ZMC datum are provided. Finally, the transformation relationship of the three datums constraints is derived.

2.1 Observation model

The raw observation equation of the code P and carrier phase L can be expressed as follows:

$$P_{r,f}^{s} = \rho_r^s + c(t_r - t^s) + c\left(d_{r,f} - d_f^s\right) + \gamma_f I_{r,1}^s + m_r^s \cdot Z_r + e_{r,f}^s \quad (1)$$

$$L_{r,f}^{s} = \rho_r^s + c(t_r - t^s) + \lambda_f\left(B_{r,f} - B_f^s\right) - \gamma_f I_{r,1}^s + \lambda_f N_{r,f}^s + m_r^s \cdot Z_r + \varepsilon_{r,f}^s \quad (2)$$

wherein r and s represent the receiver and satellite, respectively, f refers to the different frequency bands, ρ_r^s is the geometric distance between one satellite and receiver, c is the speed of light in vacuum, and t_r and t^s are the receiver and satellite clock offsets, respectively, $d_{r,f}$ and d_f^s are the code hardware delays on the frequency f in meters of the receiver and the satellite, respectively, $B_{r,f}$ and B_f^s are the phase delays on the frequency f in cycles of the receiver and satellite, respectively, $I_{r,1}^s$ is the ionospheric delay on the first frequency, γ_f is the ionospheric coefficient for different frequencies, and it

can be expressed as $\gamma_f = f_1^2/f_n^2$, λ_f is the wavelength of the carrier phase in meters, $N_{r,f}^s$ is the carrier phase ambiguity in cycles, m_r^s and Z_r are the wet mapping function and zenith wet delay of the tropospheric delay, respectively, and $e_{r,f}^s$ and $\varepsilon_{r,f}^s$ are the measurement noise and multipath error for the code and carrier phase, respectively.

In the data processing of the dual-frequency observation model, the ionospheric-free (IF) combination is selected to calculate based on the two observations at two different frequency bands, therefore, the first-order ionospheric delay is eliminated. After the IF combination is applied, the code hardware delays of the receiver and satellite can be absorbed by the receiver and satellite clock offset, respectively. The phase hardware delays of the receiver and satellite can be absorbed by the ambiguity parameter. Therefore, the observation model can be reformulated as follows:

$$P_{r,IF}^s = \rho_r^s + c(\bar{t}_r - \bar{t}_s) + m_r^s \cdot Z_r + e_r^s \quad (3)$$

$$L_{r,IF}^s = \rho_r^s + c(\bar{t}_r - \bar{t}_s) + \lambda_{IF}\bar{N}_{r,IF}^s + m_r^s \cdot Z_r + \varepsilon_r^s \quad (4)$$

where $\bar{t}_r$ and $\bar{t}_s$ are the re-parameterized receiver and satellite clock offset, respectively. The IF combination of dual-frequency code hardware delay can be absorbed by them, and they can be expressed as $\bar{t}_r = t_r + d_{r,IF}$, $\bar{t}_s = t^s + d_{IF}^s$. Furthermore, $\bar{N}_{r,IF}^s$ is the re-parameterized float IF phase ambiguity, which absorbs the phase and code hardware delays of the receiver and satellite and can be expressed as $\bar{N}_{r,IF}^s = N_{r,IF}^s + B_{r,IF} - B_{IF}^s + d_{IF}^s - d_{r,IF}$ [Wang, et al, 2019]. It should be noted that the phase wind-up, earth rotation correction, relativistic effect, satellite antenna phase center offsets (PCO), phase center variations (PCV), solid tide and ocean tide, and pole tide are carefully considered. When the satellite clock offset estimation is conducted using the UD observation model, the satellite orbit and station coordinates are fixed. Therefore, the parameters, including the satellite and receiver clock offset, the wet delay of the tropospheric and the float ambiguities, should be estimated.

2.2 Functional model

We assume that there are q satellites observed by u stations, and m pseudorange and m carrier phase observations in total at an epoch. According to observation models (3) and (4), $P_{r,IF}^s$ and $L_{r,IF}^s$ on the left side of the equation are moved to the right, and the observation model can be transformed into a functional model. The satellite and receiver clock offsets are estimated as white noise, the troposphere is regarded as a constant during a period of time, and the ambiguity is also a constant for each arc if no cycle slip occurs. Therefore, the satellite and receiver clock offset parameters are placed in a matrix, and the troposphere and ambiguity parameters are fed into another matrix. The functional model based on the observation model of all stations can be expressed as:

$$\underset{2m\times 1}{V} = \underset{2m\times(u+q)}{A}\ \underset{(u+q)\times 1}{X_1} + \underset{2m\times(u+m)}{B}\ \underset{(u+m)\times 1}{X_2} - \underset{2m\times 1}{L} \quad (5)$$

where V denotes the residuals vector, A is the coefficient matrix of receiver and satellite clock offset, X_1 is the satellite and receiver clock offset parameter vector. B is the coefficient matrix of the troposphere and ambiguity, X_2 is the troposphere and the ambiguity parameter vector, and L is the observation vector of the code and carrier phases. Then, the normal equation can be expressed as follows:

$$MX = W \quad (6)$$

where $M = \begin{bmatrix} A^TPA & A^TPB \\ B^TPA & B^TPB \end{bmatrix}$, $X = \begin{bmatrix} X_1 \\ X_2 \end{bmatrix}$ and $W = \begin{bmatrix} A^TPL \\ B^TPL \end{bmatrix}$.

It is noted that there is a linear dependency between the receiver and the satellite clock offset, resulting in rank deficiency, whose number is 1 in the M matrix, resulting in (6) cannot be determined. Therefore, one clock offset datum should be selected to eliminate the rank deficiency, and then the receiver and satellite clock offset can be separated.

2.3 A satellite as clock offset datum

The clock offset value of one satellite is set as zero for each epoch when the clock offset datum is one satellite. Assuming that the clock offset of the q^{th} satellite is zero, it can be expressed as follows:

$$\bar{t}_s^q = 0 \quad (7)$$

where q is the order of the clock offset datum satellite among all of satellites. According to the

constraints condition, it can be expressed in the following matrix form:

$$\begin{cases} K_{s\ 1\times(u+q+u+m)} \cdot X_{(u+q+u+m)\times 1} = 0 \\ K_{s\ 1\times(u+q+u+m)} = [0,0,\dots,0,0\dots 0,1,\underset{u+u+m}{0}] \end{cases} \quad (8)$$

According to the adjustment of indirect observations with the constraints model, and combining (6) and (8), the matrix M can be reformulated as:

$$M = M + K_s^T K_s \quad (9)$$

Then, the rank deficiency of the matrix M can be eliminated, and the satellite clock offset can be estimated with the satellite clock datum.

2.4 A receiver as clock offset datum

The clock offset value of one receiver is set to zero when the clock offset datum is one receiver. Assuming the u^{th} receiver clock offset is zero, it can be expressed as follows:

$$\bar{t}_r^u = 0 \quad (10)$$

where u is the order of the clock offset datum receiver among all of receivers. According to the constraints condition, it can be expressed in the following matrix form:

$$\begin{cases} K_{r\ 1\times(u+q+u+m)} \cdot X_{(u+q+u+m)\times 1} = 0 \\ K_{r\ 1\times(u+q+u+m)} = [\underset{q+u+m}{0},0,0,\dots,0,0,0\dots\dots 1] \end{cases} \quad (11)$$

where the element '1' is the 1st row and $(q+u+m+u)^{\text{th}}$ column in the K_r vector. According to the adjustment of indirect observations with the constraints model, combining (6) and (11), the matrix M can be reformulated as:

$$M = M + K_r^T K_r \quad (12)$$

Then, the rank deficiency of the matrix M can be excluded, and the satellite clock offset can be estimated with the receiver clock datum.

2.5 ZMC as clock offset datum

The mean value of all satellite clock offsets is set as zero when the clock offsets datum is ZMC, and it can also be expressed as the sum value of all satellite clock offsets being zero, which can be expressed as:

$$\sum_{n=1}^{q} dt^n = 0 \quad (13)$$

where n is the number of satellites. According to the constraints condition, it can be expressed in matrix form:

$$\begin{cases} K_{z\ 1\times(q+u+u+m)} \cdot X_{(q+u+u+m)\times 1} = 0 \\ K_{z\ 1\times(u+q+u+m)} = [\underset{1\times q}{e}, \underset{1\times(u+u+m)}{0}] \\ \underset{1\times q}{e} = [1,1,\dots 1] \end{cases} \quad (14)$$

where the elements of K_z from the 1st column to the q^{th} column are '1'. According to the adjustment of indirect observations with the constraints model and combining (6) and (14), the matrix M can be reformulated as

$$M = M + K_z^T K_z \quad (15)$$

Then, the rank deficiency of the matrix M can be excluded, and the satellite clock offset can be estimated with the ZMC datum.

2.6 Transformation relationship analysis of three datum restraints

It can be seen from (8), (11), and (14) when different clock offset datum constraints are applied to satellite clock offset estimation, their difference is the constraint condition. After selecting the clock offset datum, the estimated parameter matrix can be expressed as

$$X_s = (M + K_s K_s^T)^{-1} W = Q_s W \quad (16)$$

$$X_r = (M + K_r K_r^T)^{-1} W = Q_r W \quad (17)$$

$$X_z = (M + K_z K_z^T)^{-1} W = Q_z W \quad (18)$$

where, X_s, X_r, and X_z are estimated parameter matrices based on the satellite clock offset datum, receiver clock offset datum, and ZMC datum, respectively. Q_s, Q_r, and Q_z are the cofactor matrices for the satellite clock offset datum, receiver clock offset datum, and ZMC datum, respectively. According to (11), (16), and (17), the relationship between X_s and X_r can be expressed as:

$$X_s = Q_s W = Q_s (M + K_r K_r^T) X_r = Q_s M X_r \quad (19)$$

Considering that the vector K_s is rank deficiency, and the matrix M and the constraints condition (K_s, K_r, K_z) are not linearly dependent, therefore $MK_s = MK_r = MK_z = 0$. Then, $Q_s K_s$ can be expressed as:

$$Q_s K_s = Q_s M K_s (K_s^T K_s)^{-1} + Q_s K_s K_s^T K_s (K_s^T K_s)^{-1} \quad (20)$$

$$Q_s K_s = (Q_s M + Q_s K_s K_s^T) K_s (K_s^T K_s)^{-1} = K_s (K_s^T K_s)^{-1} \quad (21)$$

Therefore, the $Q_s M$ can be expressed as:

$$Q_s M = Q_s (M + K_s K_s^T - K_s K_s^T) = I - K_s K_s^T = I - K_s (K_s^T K_s)^{-1} K_s^T \quad (22)$$

Then, the relationship between X_s and X_r can be expressed as:

$$X_s = [I - K_s (K_s^T K_s)^{-1} K_s^T] X_r \quad (23)$$

Therefore, the satellite clock offset can be transformed from the receiver clock datum to the satellite clock datum by using the K_s vector and the clock offset with the receiver clock datum. Similarly, the relationship between X_s and X_z, X_r, and X_z can also be transformed.

3 Characteristics of three datums constraints

Three datum constraints can be theoretically transformed. In fact, the clock offset datum noise, frequency stability, and applicable conditions for different clock offset datums are different. Therefore, the characteristics of three clock offset datums are analyzed in this section.

The receiver clock offset value is constrained to zero for each epoch when the clock offset datum is one receiver, and the remaining satellites and receiver clock offset are estimated with respect to this clock offset datum. The advantage is that it can ensure that all satellite clock offsets have a value and this value is not equal to zero, which is beneficial to all satellite clock performance monitoring and all satellite clock performance can be evaluated by using the satellite clock offset. The disadvantage is that one receiver clock offset value is set as zero, which can negatively impact the performance evaluation of this receiver clock. Furthermore, during real-time satellite clock offset estimation, the observation data of the clock offset datum receiver cannot be received by the user owing to the network delay of real-time observation data transmission, temporary modem failure [EI-Mowafy, et al, 2017], or other factors. There is no observation data in the clock offset datum receiver, and the satellite clock offset cannot be estimated at that time. To ensure that the satellite clock offset can be estimated continuously, the clock offset datum should be changed into another receiver. However, all of satellite clock offset values would jump almost the same amount at that time. If this clock offset is used for frequency stability estimation and modeling of the satellite clock offset, the performance of the satellite clock cannot be reflected due to the clock offset jump, which is not good for satellite clock performance evaluation, and the modeling of the satellite clock offset is also inaccurate. When each epoch of the clock offset datum receiver has observation data, one receiver clock can be used as a clock offset datum for the clock offset estimation. Furthermore, when regional network stations are used for real-time satellite clock estimation, it is appropriate that the receiver clock is selected as the datum.

When the clock offset datum is one satellite clock, one satellite clock offset value is constrained to zero for each epoch. All receiver clock offset values can be reserved under these circumstances, which is beneficial for the performance evaluation of the receiver clock. The drawback is that one satellite clock offset value is zero, which is unfavorable for all satellite clock performance monitoring and evaluation. When the clock offset is estimated, the receiver clock offset needs to be reserved, and one satellite clock offset value is zero does not affect its application, this datum can be recommended.

When the real-time satellite clock offset is estimated and the clock offset datum is ZMC, the mean value of all satellite clock offsets is zero. Therefore, all satellite and receiver clock offset values are not zero, which is beneficial to all satellite and receiver clock performance evaluations. Furthermore, because all satellites and receiver clock offset values are not equal to zero, the satellite and receiver clock noise can be absorbed by itself. However, the satellite signal cannot be tracked by any receiver on the ground owing to the signal loss of lock or other failures, as shown in Figure 1. It can be seen that C07 satellite clock offset experienced data disruption at 13:44:30 because the C07 satellite could not be tracked by all stations. Under this condition, the satellite clock offset jump occurred, and the satellite clock offset data was discontinuous, which is not suitable for all satellite clock performance evaluations. A short-term clock

offset prediction [El-Mowafy et al. 2017, Zhao et al. 2020] of the C07 satellite clock may guarantee the continuity of all satellite clock offsets. The ZMC datum is suitable when the satellite and receiver clock offset must be reserved. Furthermore, when the number of estimated satellite clock offsets of all epochs are the same, the ZMC datum is also suitable.

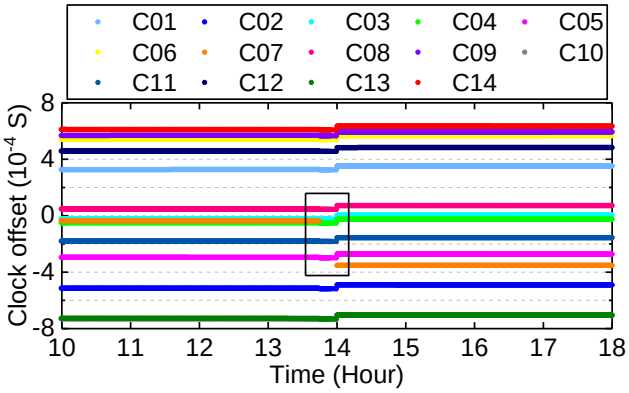

Fig.1 Time series of BDS satellite clock offset

4 Experiments and results

In this section, the data and processing strategy are described first. Then, the frequency stability of the clock offset datum is analyzed. Thereafter, the clock performance of the three datum constraints is evaluated in terms of clock offset accuracy, clock offset model precision, frequency stability, and PPP.

4.1 Data and processing strategy

The BDS-2 was selected to conduct the experiment. The simulated real-time satellite clock offset estimation is applied. The 100 observation stations from IGS Multi-GNSS Experiment (MGEX) network [Montenbruck et al. 2017] evenly distributed all over the world were used to estimate the BDS satellite clock offset products. And the BDS signal can be tracked by all of them. Figure 2 shows the geographic distribution of the stations. The red dots indicate the stations used to estimate clock offset, while the blue triangles mean the stations applied for perform RT-PPP. The experiment was simulated in real-time mode, and the clock offset estimation was carried out from 31 March to 6 April 2019 (DOY 090–096) by using the rtclk (Real-Time Clock) software developed by BeiDou Analysis and Service Center of Chang'an University [Fu et al. 2019]. In the process of clock offset estimation, observations with B1/B2 frequency and 30 s sample rate were applied, the elevation mask was set to 7°, and the GBM final orbit products were used [Deng et al. 2014]. For quality control, when one residual of observation was larger than 8.5 times the median of normalized residuals, this residual with respect to the observation data was deleted [Fu et al. 2018]. The details of the data process strategy for clock offset estimation can be found in Table 1.

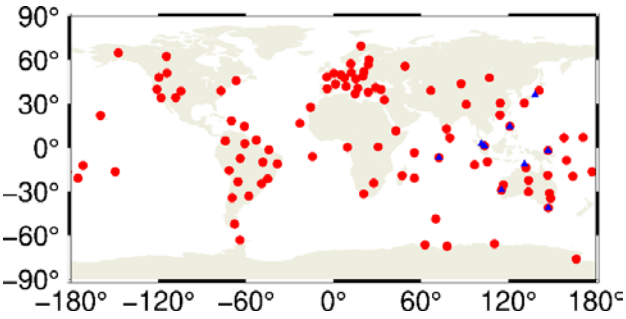

Fig. 2 Geographic distribution of stations. The red points denote 100 stations are used for clock offset estimation, the blue triangle denote 10 stations are applied for PPP

To compare the satellite clock performance with three different datum constraints, three schemes were designed for comparisons, which are as follows:

Scheme 1: BDS real-time satellite clock estimation using the TID1 receiver clock offset as datum. Scheme 2: BDS real-time satellite clock estimation using the C08 satellite clock offset as datum. Scheme 3: BDS real-time satellite clock estimation and the clock offset datum imposed on ZMC datum of all satellite clock. It is noted that for different constraints, the clock offset processing of GEO/IGSO/MEO satellite are treated as the same.

4.2 Clock offset datum stability analysis

The frequency stability is used to describe the random fluctuation of the atomic clock output frequency caused by noise. The overlapping Hadamard deviation and overlapping Allan deviation were selected to evaluate the frequency stability of the rubidium atomic clock and the passive hydrogen maser (PHM), respectively. Based on the clock offset data, overlapping Hadamard deviation and overlapping Allan deviation can be expressed as follows [Riley

2007]:

$$H\sigma_y(\tau) = \sqrt{\frac{1}{6(N-3m)\tau^2}\sum_{k=1}^{N-3m}[x_{k+3m} - 3x_{k+2m} + 3x_{k+m} - x_k]^2} \quad (24)$$

$$H\sigma_y(\tau) = \sqrt{\frac{1}{2(N-2m)\tau^2}\sum_{k=1}^{N-2m}[x_{k+2m} - 2x_{k+m} + x_k]^2} \quad (25)$$

where $H\sigma_y(\tau)$ indicates the frequency stability, N is the number of clock offset data, m is the smooth factor, and τ is the smooth time.

Table 1 Data process strategy for BDS real-time clock estimation

Items	Strategy
Observations	Ionospheric-free (IF) combination
Signal selection	B1/B2
Sampling rate	30 s
Elevation mask	7°
Weight	1 when E>30°; 2sin(E) for E<30°
Estimator	Sequential least squares
Satellite orbit	Fixed to the GBM final orbit
Satellite antenna phase center and variation	ESA model [Dilssner et al. 2014]
Phase wind-up effect	Corrected [Wu et al. 1993]
Relativistic effect	Corrected
Station coordinate	Fixed to the IGS weekly solution
Station displacement	Solid earth tide, pole tide, ocean tide
Receiver antenna phase center and variation	igs14.atx
Satellite clock	Estimated as white noise
Receiver clock	Estimated as white noise
Tropospheric delay	Saastamoinen model and GMF mapping functions, estimated every one hour
Phase ambiguities	Constants for each continuous tracking arc
Clock offset datum	TID1 receiver clock / C08 satellite clock / ZMC

Maciuk [2009] has demonstrated that the frequency stability of the satellite clock using the clock offset datum receiver equipped with a hydrogen-maser clock is better than that of the internal and cesium atomic clock when conducting satellite clock estimation. There is a close correlation between the reference clock and the frequency stability of the estimated clock offset. Therefore, when the satellite clock offset estimation is based on the receiver clock offset datum, the receiver equipped with a hydrogen-maser clock is usually selected to ensure a high-precision satellite clock. It should be noted that in this study, the TID1 station was equipped with an external H-maser and a rubidium atomic clock installed on the C08 satellite clock during the experiment [Han et al. 2011]. The frequency stability of the TID1 receiver and C08 satellite clock was evaluated using IGS and GBM rapid products, respectively. The mean sub-daily frequency stability of the C08 satellite clock and TID1 receiver clocks was evaluated using overlapping Hadamard deviation and overlapping Allan deviation methods, respectively, and it is presented in Figure 3. It was observed that the frequency stability of TID1 receiver clock was significantly better than that of C08 satellite clock, and the frequency stability of the receiver clock was about one order of magnitude higher than that of the C08 satellite clock.

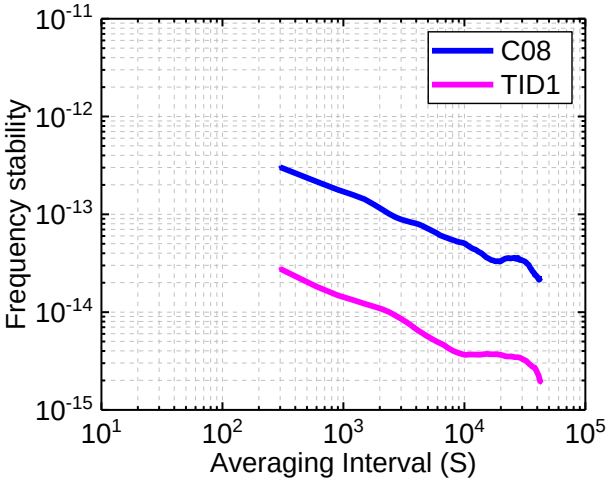

Fig. 3 The mean sub-daily frequency of the C08 satellite and TID1 receiver clock

4.3 Satellite clock offset accuracy

To evaluate the quality of the estimated satellite clock

with three different clock offset datum, the clock offset accuracy is compared to the GBM final clock products because the satellite orbit is fixed to the GBM when estimating BDS real-time satellite clock offsets. The standard IGS clock offset evaluation procedure is adopted, in which the STD and root mean square (RMS) are applied to assess the clock quality. The STD indicates the values of the processing quality of the phase observations and shows the quality of the clock solution, while the RMS values can reflect the consistency between code and phase observations, which shows the accuracy of code observations [Ge et al. 2012; Liu et al. 2019].

The experiment was conducted from DOY 090 to 096, 2019; considering that the convergence time in DOY 090 and the C07 satellite experienced the loss of lock in DOY 095, the result can be impacted by the ZMC datum [Odijk et al. 2016]. Therefore, the results of DOY 090 and 095 have been excluded. The mean STD and RMS of the BDS satellite clock with three datum constraints are shown in figure 4. For the three datum constraints, it can be seen that STD is better than 0.2, 0.1, and 0.25 ns for GEO, IGSO, and MEO satellite clock offset, respectively. In terms of the RMS, the GEO, IGSO, and MEO satellite clock offset are better than 1.0, 0.5, and 2.0 ns. The poor STD and RMS of the MEO satellite clock offset can be attributed to the fact that the observation stations tracked by the BDS satellite are limited around the world. Compared to the IGSO satellite, the relatively poor STD and RMS of the GEO satellite clock is due to the weak geometry strength of the GEO satellite orbit compared to that of the IGSO; and geometry observation conditions change slowly, resulting in the decreased orbit accuracy of the GEO satellite compared to the IGSO satellite, which then impacts the clock offset estimation accuracy [Liu et al. 2017; Zhao et al. 2013].

The mean STD and RMS for GEO, IGSO, and MEO satellite clock with three datum constraints are shown in Table 2. For the STD, the value between the TID1 and ZMC datum shows almost the same value for the GEO satellite clock, the difference is 0.002 ns which can be neglected. However, the STD is the worst for the GEO satellite clock when the clock offset datum is the C08 satellite clock. For the IGSO and MEO satellite clock, the STD with TID1 receiver clock datum and C08 satellite clock datum is almost identical, and the clock offset accuracy with the ZMC datum is slightly better than the TID1 receiver and C08 satellite clock. For the RMS, the ZMC datum shows the best accuracy regardless of whether it is GEO, IGSO, or MEO satellite, and the RMS of GEO, IGSO, and MEO satellite clock offset is 0.449, 0.177, and 0.787 ns, respectively. Compared to the TID1 receiver clock datum, the improvements in clock accuracy are 27.11%, 45.54%, and 44.07% for the GEO, IGSO, and MEO satellite clock, respectively. The improvement is 30.50%, 10.61%, and 41.00% for GEO, IGSO, and MEO satellite clock when compared to the C08 satellite clock datum, respectively. Therefore, it can be inferred that the consistency between code and phase observations of the ZMC is better than the TID1 receiver and C08 satellite clock datum.

For real-time satellite clock estimation with three datum constraints, the mean STD is 0.118, 0.124, and 0.101 ns for the TID1 receiver clock, C08 satellite clock, and ZMC datum, respectively. In terms of RMS, the mean RMS is 0.661, 0.646, and 0.405 ns with TID1 receiver clock, C08 satellite clock datum, and ZMC datum, respectively. The mean differences of STD and RMS between the TID1 receiver and C08 satellite clock datum are 0.006 and 0.015 ns, which shows that these two datum constraints have the same comparable clock offset accuracy. However, the STD and RMS of the ZMC show better performance. It has been demonstrated that three datum constraints can be theoretically transformed, and the clock offset accuracy should be the same for three different clock offset datum. However, when the clock offset datum is the receiver or satellite clock, the clock offset datum is set as zero [Liu et al. 2019; Loyer et al. 2012], the clock offset datum noise can be absorbed into other receiver or satellite clock, resulting in a decrease in the accuracy of the satellite clock offset, and therefore, there is a clock offset accuracy difference for the different clock offset datum. For the ZMC datum, all satellite and receiver clock offsets can be estimated, and all clock offsets are not equal to zero, thus the clock noise can be decreased and the clock accuracy

can be improved. Therefore, the STD and RMS with ZMC are better than those of the TID1 receiver and C08 satellite clock offset datum.

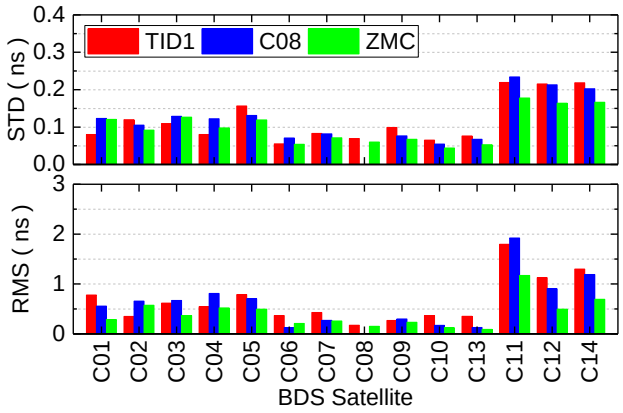

Fig.4 STD and RMS of each BDS satellites with three datums constraints

Table 2 Clock offset accuracy of BDS GEO, IGSO and MEO satellites with three datums constraints

	STD			RMS		
	TID1	C08	ZMC	TID1	C08	ZMC
GEO	0.109	0.122	0.111	0.616	0.646	0.449
IGSO	0.075	0.070	0.058	0.325	0.198	0.177
MEO	0.218	0.217	0.169	1.407	1.334	0.787

4.4 Satellite clock offset model precision

The satellite clock offset model precision is also called fitting precision, which is the RMS of the fitting residuals of the satellite clock offset model, and it can reflect the noise level characteristics of the atomic clock, which can directly determine the accuracy and stability of real-time clock offset prediction and estimation [Huang et al. 2013]. Therefore, the satellite clock offset model precision is selected to evaluate the clock quality. The rubidium atomic clocks are equipped on the BDS-2 satellites [Han et al. 2011], and the frequency drift is apparent. Therefore, the quadratic polynomial model was employed to fit the daily clock offset. The RMS is applied to express the noise level, and it can be expressed as follows:

$$x_k = a_0 + a_1(t_k - t_0) + \frac{1}{2}a_2(t_k - t_0)^2 + \varepsilon_k \quad (26)$$

$$RMS_p = \sqrt{\frac{1}{n}\sum_{k=1}^{n}\varepsilon_k^2} \quad (27)$$

where x_k is clock offsets; a_0, a_1 and a_2 are the phase, frequency, and frequency drift, respectively; t_k and t_0 are the observation and reference epochs, respectively; ε_k is the fitting residuals, which is the difference between the satellite clock offset value and the satellite clock offset model value for each epoch [Xie et al. 2019]. After ε_k is calculated, the clock offset model precision can be obtained.

The mean satellite clock offset model precision of each BDS satellite clock with three datum constraints is shown in figure 5. For the GEO satellite clock, the satellite clock offset model precision is almost the same when the TID1 receiver clock and ZMC are used as clock offset datum, while the satellite clock offset model precision of C08 satellite clock datum is significantly worse than that of the TID1 receiver clock datum and ZMC datum. The clock offset model precision of the TID1 receiver clock datum shows the poorest performance among the three datum constraints for the IGSO satellite clock, and there is a small difference in clock offset model precision between the ZMC and C08 satellite clock datum. For the MEO satellite clock, the ZMC datum shows the best clock offset model precision among the three datum constraints. The values for the C11, C12, and C14 satellite clocks are 0.357, 0.227, and 0.244 ns, respectively. The clock offset model precision with TID1 receiver clock datum is slightly worse than that of the ZMC datum, the worst satellite clock offset model precision is the C08 satellite clock datum. Overall, the mean satellite clock offset model precision is 0.497, 0.580, and 0.442 ns for the TID1 receiver clock, C08 satellite clock, and ZMC datum, respectively, and this difference is small. Compared to the TID1 receiver and C08 satellite clock datum, the satellite clock offset model precision can be improved by approximately 11.06% and 23.79% when the ZMC datum is used. Therefore, when estimating BDS real-time clock offset, the clock offset datum using the ZMC method is more suitable for modeling the satellite clock offset.

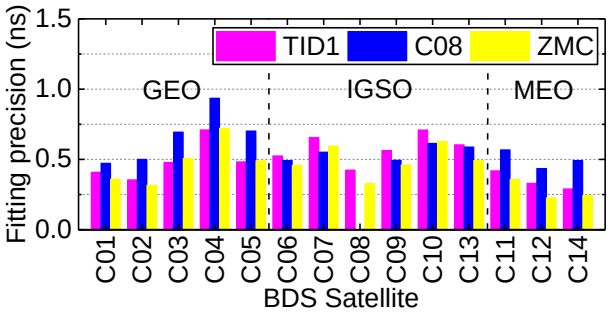

Fig. 5 The mean fitting precision of each BDS satellites with three datums constraints

4.5 Frequency stability

The mean sub-daily frequency stability of the satellite clock for five days with the three datum constraints is shown in Figure 6. The sub-daily frequency stability shows almost the same variation trends among the three datum constraints, which indicates that clock frequency stability variation is not impacted by the clock offset datum. Furthermore, the visible 'bump' has appeared for C11 satellite clock at an integration times of 2,000 s, which can be attributed to the impact of the special period existed in the C11 satellite clock offset. The special period may be caused by the hardware noise of its atomic clock [Huang et al. 2018, Wang et al. 2016]. Furthermore, the frequency stability decreases when the integration time exceeds 10,000 s for some GEO and IGSO satellite clocks, such as C04, C07, and C10 satellite clocks, which can also be attributed to the impact of periodic terms.

For integration times of 100 s, 1000 s, 10000 s, and 20000 s, the frequency stability of the different clock offset datums is shown in Figure 7. It can be seen that when the averaging interval time is 100 s, the frequency stability with the C08 satellite clock datum exhibits the poorest performance. The satellite clock frequency stability with the ZMC datum is slightly better than that with the TID1 receiver clock offset datum.

When the averaging interval is 1000 s, the mean frequency stability is 1.15×10^{-13}, 2.06×10^{-13}, and 1.09×10^{-13} for GEO satellite with the TID1 receiver clock datum, C08 satellite clock, and ZMC datum, respectively. As for IGSO satellite clock, the mean frequency stability is 1.79×10^{-13}, 2.51×10^{-13}, and 1.68×10^{-13} for TID1 receiver clock datum, C08 satellite clock datum, and ZMC datum, respectively. For the MEO satellite clock, the mean frequency stability with the TID1 receiver clock datum, C08 satellite clock datum, and ZMC datum is 1.51×10^{-13}, 2.31×10^{-13}, and 1.41×10^{-13}, respectively. The GEO satellite clock presents the best performance, and the frequency stability with the ZMC datum shows the best performance.

When the averaging interval is 10000 s, the mean frequency stability for GEO, IGSO, and MEO satellite clock is 5.62×10^{-14}, 7.64×10^{-14}, and 5.57×10^{-14} with TID1 receiver clock datum, 6.68×10^{-14}, 8.02×10^{-14}, and 6.17×10^{-14} for the C08 satellite clock datum, 4.31×10^{-14}, 5.88×10^{-14}, and 3.63×10^{-14} for the ZMC datum, respectively. Compared to the TID1 receiver clock and C08 satellite clock, the frequency stability with the ZMC datum can be improved by 23.34%, 23.04%, 34.84% and 35.40%, 26.63%, and 41.13% for GEO, IGSO, and MEO satellite clock, respectively. Moreover, the frequency stability performance of the MEO satellite clock is better than that of the GEO and IGSO satellite clocks.

When the integration time is longer than 10000 s, the frequency stability variation is more complex. Previous studies have demonstrated that the periodic terms exist in the BDS satellite clock offset [Wang et al. 2016], and the frequency stability is impacted by this periodic terms when the integration time is longer than 10000 s. The degree of frequency stability of each satellite clock affected by periodic terms is still unknown, and it should be studied in the future. When the averaging interval is less than 10000 s, the frequency stability difference can be attributed to the difference in clock datum frequency stability.

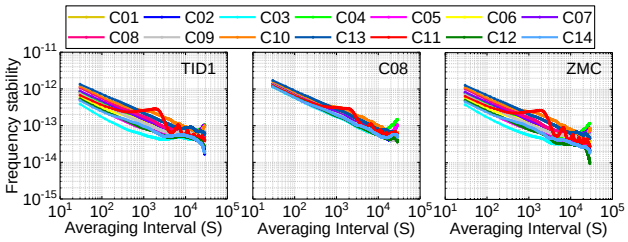

Fig. 6 Sub-daily frequency stability of each BDS satellites with three datum constraints

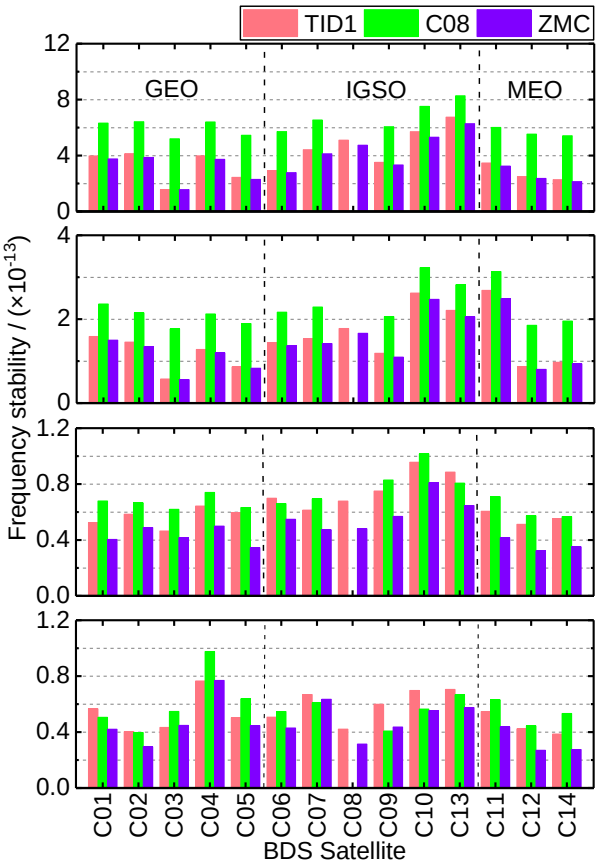

Fig. 7 Frequency stability of each BDS satellite clock

4.6 PPP

One of the applications of real-time estimated satellite clock offset is in RT-PPP. To analyze the difference in satellite clock performance with three datum constraints, the BDS kinematic PPP is conducted by using three different clock offset products. Furthermore, PPP using GBM final clock offset products is also performed for comparison. For PPP, 10 stations are selected to conduct the PPP (figure 2). Among them, four stations are involved in the clock offset estimation, while another six are not. The sample rate of observations is 30 s, the satellite orbit is GBM final orbit, and the ambiguity is set as a float solution. The observation data are from DOY 091 to 096, 2019, except for DOY 095, 2019. The RMS is calculated after PPP convergence, and the mean RMS for each station is shown in figure 6.

For most stations, the BDS kinematic PPP accuracy in the east, north, and up components present almost the same performance for the three datum constraints, ranging from 7 to 14 cm, 4 to 11 cm, and 14 to 28 cm, respectively. Due to the poor accuracy of the GEO satellite orbit, the accuracy of BDS kinematic PPP is poorer than that of GPS [Zhou et al. 2020]. However, with the construction of BDS-3, the PPP accuracy can be significantly improved in the future [Jiao et al. 2019]. The mean PPP accuracy of ten stations with the three datum constraints and GBMs are presented in Table 3. The mean PPP accuracies in the east, north, and up directions are 10.51, 6.67, and 21.51 cm with the TID1 receiver clock datum, 11.97, 6.76, and 21.08 cm with C08 clock datum, and 10.82, 6.58, and 20.08 cm with ZMC datum, respectively. ZMC datum shows better positioning performance among the three datum constraints. Considering that the STD of the clock accuracy of the three clock offset datums is between 0.101 and 0.121 ns, the difference between the three datum constraints and GBM is within the normal range.

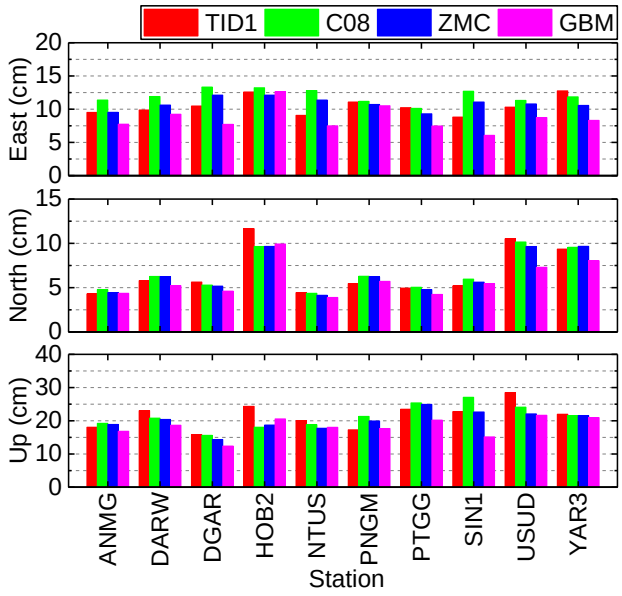

Fig. 8 RMS of BDS kinematic PPP in east, north and up for each station

Table 3 Mean PPP accuracy with three datums and GBM (units: cm)

	TID1	C08	ZMC	GBM	GBM-TID1	GBM-C08	GBM-ZMC
East	10.51	11.97	10.82	8.66	1.85	3.31	2.16
North	6.67	6.76	6.58	5.88	0.79	0.88	0.70
Up	21.51	21.08	20.08	18.29	3.22	2.79	1.79

5 Conclusions

This study presents the BDS real-time satellite clock offset estimation with three datum constraints, including one receiver clock, one satellite clock, and ZMC. It proves that the three datum constraints can be theoretically transformed. Furthermore, the characteristics of the three datum constraints were analyzed. The receiver clock is recommended as the clock offset datum under the following conditions: the clock offset datum of each epoch has observation data, and the regional stations network is used to estimate the real-time satellite clock offset. If all the receiver clock offsets are reserved and one satellite clock offset value being zero does not affect the application of the satellite clock offset, one satellite can be used as a clock offset datum. When the number of satellite clocks of all epochs is the same and the stations are globally distributed, the ZMC datum is suitable.

To compare the clock offset quality of the three datum constraints, 100 stations from the MGEX network are used to estimate the BDS real-time satellite clock. The BDS satellite clock performance with three datum constraints is evaluated in terms of clock offset accuracy, fitting precision, frequency stability, and PPP. For clock offset accuracy, the mean STD is 0.118, 0.124, and 0.101 ns for the clock offset datum for the TID1 receiver clock, C08 satellite clock, and ZMC datum, respectively. The mean RMS is 0.661, 0.646, and 0.405 for the TID1 receiver clock datum, C08 satellite clock datum, and ZMC, respectively. The mean fitting precision of the TID1 receiver clock datum, C08 satellite clock datum, and ZMC are 0.497, 0.580, and 0.442 ns, respectively. As for the frequency stability, when the integration is less than 10000 s, the clock offset datum with ZMC shows better performance. In terms of PPP, the ZMC shows better positioning performance among three datum constraints. The reason for the numerical difference among the three datum constraints can be attributed to the difference in frequency stability for the satellite and receiver clock. For the ZMC datum, all satellites and receiver clock offsets can be estimated, and the satellite and receiver clock noise can be absorbed. Therefore, clock performance is better.

Acknowledgments

The IGS, IGS-MGEX, GBM are greatly acknowledged for providing the Multi-GNSS tracking data, sinex coordinates, erp, satellite orbit and clock products. This work was funded by the Programs of the National Natural Science Foundation of China (41774025, 41731066, 41904038) , the National Key R&D Program of China (2018YFC1505102), the Special Fund for Technological Innovation Guidance of Shaanxi Province (2018XNCGG05), the Special Fund for Basic Scientific Research of Central Colleges (grant no. CHD300102269305, CHD300102268305, Chang'an University), and the China Postdoctoral Science Foundation (2019M662713), and the Grand Projects of the Beidou-2 System (GFZX0301040308), the Fundamental Research Funds for the Central Universities, CHD(300102261713).

Data Availability

BDS precise ephemeris was retrieved from: ftp://ftp.gfz-potsdam.de/pub/GNSS/products/mgnss. BDS raw observations from MGEX stations were retrieved from: ftp://cddis.gsfc.nasa.gov/pub/gnss/data/daily/.

References

Bock, H.; Hugentobler, U.; Springer, T.A. and Beutler, G. (2002): Efficient precise orbit determination of LEO satellites using GPS, Adv. Space Res. 30(2), 295–300.

Chen, L.; Zhao, Q.; Hu, Z.; Jiang, X.; Geng, C., Ge, M. and Shi, C. (2018): GNSS global real-time augmentation positioning Real-time prototype system construction and performance analysis, Adv Space Res 61(1): 367-384.

Defraigne, P.; Aerts, W. and Pottiaux, E. (2015): Monitoring of UTC(k)' s using PPP and IGS real-time products, GPS Solutions 19(1): 165-172.

Deng, Z.; Ge, M.; Uhlemann, M; and Zhao, Q. (2014): Precise orbit determination of BeiDou satellites at GFZ, In: Proceedings of IGS workshop 2014, 23–27 June 2014, Pasadena, USA.

Dilssner, F.; Springer, T.; Schonemann, E.; Enderle, W. (2014): Estimation of satellite antenna phase center corrections for BeiDou. In: Proceedings of

IGS workshop 2014, June 23-27, Pasadena, USA

El-Mowafy, A.; Deo, M.; Kubo, N. (2017): Maintaining real-time precise point positioning during outages of orbit and clock corrections. GPS Solutions 21(3): 937–947.

Fu, W.; Huang, G.; Zhang, Q.; Gu, S.; Ge, M.; Schuh, H. (2019): Multi-GNSS real-time clock estimation using sequential least square adjustment with online quality control. Journal of Geodesy 93(7): 963–976.

Fu, W.; Yang, Y.; Zhang, Q.; Huang, G. (2018): Real-time estimation of BDS/GPS high-rate satellite clock offsets using sequential least squares. Adv Space Res 62(2): 477-487.

Ge, M.; Chen, J.; Douša, J.; Gendt, G.; Wickert, J. (2012): A computationally efficient approach for estimating high-rate satellite clock corrections in real-time. GPS Solutions 16(1):9–17.

Guo, J.; Li, X.; Li, Z,; Hu, L.; Yang, G.; Zhao, C.; Fairbairn, D.; Watson, D.; Ge, M. (2018): Multi‐GNSS precise point positioning for precision agriculture. Precision Agriculture 19(5):895–911.

Han, C.; Yang, Y.; Cai, Z. (2011): BeiDou Navigation Satellite System and its time scales. Metrologia 48: S213–S218.

Huang, G.; Cui, B.; Zhang, Q.; Fu, W.; Li, P. (2018): An Improved Predicted Model for BDS Ultra-Rapid Satellite Clock Offsets. Remote Sens 10: 60.

Huang, G.; Zhang, Q.; Li, H.; Fu, W. (2013): Quality variation of GPS satellite clocks on-orbit using IGS clock products. Adv Space Res 51(6): 978–987.

Jiang, X.; Gu, S.; Li, P.; Ge, M.; Schuh, H. (2019): A Decentralized Processing Schema for Efficient and Robust Real-time Multi-GNSS Satellite Clock Estimation. Remote Sens. 11: 2595.

Jiao, G.; Song, S.; Ge, Y.; Su, K.; Liu, Y. (2019): Assessment of BeiDou-3 and Multi-GNSS Precise Point Positioning Performance. Sensors. 19:2496.

Liu, T.; Yuan, Y.; Zhang, B.; Wang, N.; Tan, B.; Chen, Y. (2017): Multi-GNSS Precise Point Positioning (MGPPP) using raw observations. Journal of Geodesy 91(3):253–268.

Liu, T.; Zhang, B.; Yuan, Y.; Zha, J.; Zhao, C. (2019): An efficient undifferenced method for estimating multi-GNSS high-rate clock corrections with data streams in real time. Journal of Geodesy 93(9): 1435–1456.

Loyer, S.; Perosanz, F.; Mercier, F.; Capdeville, H.; Marty, H. (2012): Zero-difference GPS ambiguity resolution at CNES–CLS IGS Analysis Center. Journal of Geodesy 86(11): 991–1003.

Lu, C.; Li, X.; Nilsson, T.; Ning, T.; Heinkelmann, R.; Ge, M.; Glaser, S.; Schuh, H. (2015): Real-time retrieval of precipitable water vapor from GPS and BeiDou observations. Journal of Geodesy 89(9): 843–856.

Maciuk, K. (2019): Satellite clock stability analysis depending on the reference clock type. Arabian Journal of Geosciences 12: 28.

Montenbruck, O.; Steigenberger, P.; Prange, L.; Deng, Z.; Zhao, Q.; Perosanz, F.; Romero, L.; Noll, C.; Sturze, A.; Weber, G.; Schmid, R.; MacLeod, K.; Schaer, S. (2017): The Multi-GNSS Experiment (MGEX) of the International GNSS Service (IGS)-Achievements, prospects and challenges. Adv Space Res 59(7): 1671-1697.

Odijk, D.; Zhang, B.; Khodabandeh, A.; Odolinski, R.; Teunissen, P J. G.; (2016): On the estimability of parameters in undifferenced, uncombined GNSS network and PPP-RTK user models by means of S-system theory. J Geod 90(1):15–44.

Riley, W. Handbook of frequency stability analysis. In Hamilton Technical Services, Beaufort; NIST Special Publicatio: Gaithersburg, MD, USA, 2007.

Wang, J.; Huang, G.; Yang, Y.; Zhang, Q.; Gao, Y.; Xiao, G. (2019): FCB estimation with three different PPP models: equivalence analysis and experiment tests. GPS Solutions 23(4):93.

Wang, B.; Lou, Y.; Liu, J.; Zhao, Q.; Su, X. (2016): Analysis of BDS satellite clocks in orbit. GPS Solutions 20(4): 783–794.

Wu, J.; Wu, S.; Hajj, GA.; Bertiger, WI.; Lichten, SM. (1993): Effects of antenna orientation on GPS carrier phase. Manuscr Geod 18(2): 91–98.

Xie, W.; Huang, G.; Cui, B.; Li, P.; Cao, Y.; Wang, H.; Chen, Z.; Shao, B. (2019): Characteristics and Performance Evaluation of QZSS Onboard

Satellite Clocks. Sensors. 19:5147.

Yang, Y.; Gao, W.; Guo, S.; Mao, Y.; Yang, Y. (2019): Introduction to BeiDou-3 navigation satellite system. NAVIGATION. 1-12.

Zhao, Q.; Guo, J.; Li, M.; Qu, L.; Hu, Z.; Shi, C.; Liu, J. (2013): Initial results of precise orbit and clock determination for COMPASS navigation satellite system. Journal of Geodesy 87(5): 475–486.

Zhou, F.; Cao, X.; Ge, Y.; Li, W. (2020): Assessment of the positioning performance and tropospheric delay retrieval with precise point positioning using products from different analysis centers. GPS Solutions 24(1):12.

Zhao, L.; Dousa, J.; Ye, S. and Vaclavovic, P. (2020): A flexible strategy for handling the datum and initial bias in real-time GNSS satellite clock estimation, Journal of Geodesy 94(1):3.

Authors

Guanwen Huang is currently a professor of Chang'an University, Xi'An, P. R. China. He received a B.Eng, M.Sc., and Ph.D. in Surveying Engineering from Chang'An University, in 2005, 2008, and 2012. His research activities include GNSS Precise Point Positioning, real-time satellite clock model, and their applications.

Wei Xie is currently a Ph,D. candidate at the College of Geology Engineering and Geomatics, Chang'An University, Xi'an, P.R. China. He completed his B.Sc. at Hunan University of Science and Technology in 2017. His research is focused on GNSS satellite clock offset estimation and satellite clock performance evaluation.

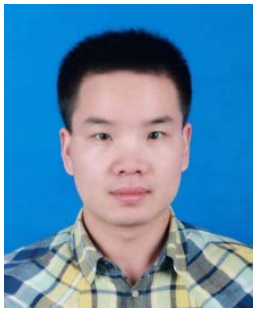

Wenju Fu received his Ph.D. from Chang'An University, Xi'An, P.R.China in 2018. He is currently a postdoctoral fellow at the State Key Laboratory of Information Engineering in Surveying, Mapping and Remote Sensing (LIESMARS), Wuhan University. His research interest includes GNSS Precise Point Positioning, precise satellite clock, and LEO applications.

Pingli Li is an engineer at the 20th Research Institute of China Electronic, Technology Group Corporation, Xi'An, P.R. China. He received his Bachelor and M.Sc. from Chang'An University in 2015 and 2018. His research focuses on GNSS precise satellite clock offset estimation.

Haohao Wang is currently a Master graduate student at the College of Geology Engineering and Geomatics, Chang'An University, Xian, P.R. China. His research focuses on GNSS real-time satellite clock offset estimation.

Fan Yue is currently a Master graduate student at the College of Geology Engineering and Geomatics, Chang'An University, Xi'an, P.R. China.